Princeton Plasma Physics Laboratory

PPPL- 4467

PPPL- 4467

Transport of Parallel Momentum by Toroidal Ion Temperature Gradient Instability near Marginality

E. S. Yoon and T. S. Hahm

October, 2009

PPPL
PRINCETON PLASMA
PHYSICS LABORATORY

Prepared for the U.S. Department of Energy under Contract DE-AC02-09CH11466.

Princeton Plasma Physics Laboratory
Report Disclaimers

Full Legal Disclaimer

Trademark Disclaimer

PPPL Report Availability

Princeton Plasma Physics Laboratory:

http://www.pppl.gov/techreports.cfm

Office of Scientific and Technical Information (OSTI):

http://www.osti.gov/bridge

Related Links:

U.S. Department of Energy

Office of Scientific and Technical Information

Fusion Links

Transport of Parallel Momentum by Toroidal Ion Temperature Gradient Instability near Marginality

E. S. Yoon and T. S. Hahm

Princeton University, Princeton Plasma Physics Laboratory, P.O. Box 451, Princeton, NJ 08543, USA

E-mail: tshahm@pppl.gov

Abstract. The turbulent angular momentum flux carried by ions resonant with toroidal ion temperature gradient(ITG) instability is calculated via quasilinear calculation using the phase-space conserving gyrokinetic equation in the laboratory frame. The results near ITG marginality indicate that the inward turbulent equipartition (TEP) momentum pinch [Hahm T.S. *et al* 2007 *Phys. Plasmas* **14** 072302] remains as the most robust part of pinch. In addition, ion temperature gradient driven momentum flux is inward for typical parameters, while density gradient driven momentum flux is outward as in the previous kinetic result in slab geometry [Diamond P.H. *et al* 2008 *Phys. Plasmas* **15** 012303].

PACS numbers: 52.30.Gz, 52.35.Qz

1. Introduction

The need for understanding momentum transport, which governs plasma rotation profile is now widely recognized. A highly anomalous level of toroidal momentum transport has persistently been observed in tokamak experiments since the early 90's [1]. Therefore, it is believed to be caused by microturbulence such as ion temperature gradient (ITG) turbulence. For instance, a comparable level of the toroidal momentum diffusivity χ_ϕ and the ion thermal diffusivity χ_i observed in Tokamak Fusion Test Reactor (TFTR) [1] experiments is in rough agreement with theoretical predictions based on ITG turbulence [2]. There is accumulating experimental evidence that momentum transport cannot be properly described by a diffusion coefficient only. This includes the identification of a nondiffusive component of the momentum flux [3], and the observation of spontaneous toroidal rotation of plasmas in the absence of apparent external torque input [4, 5, 6, 7, 8, 9, 10, 11, 12, 13]. In particular, recent perturbation experiments on JT60-U [14, 15], NSTX [16, 17], DIII-D [18] and JET [19] neutral beam heated plasmas showed the need for non-diffusive, off-diagonal momentum flux modelled as a momentum pinch to match the measured centrally peaked rotation profiles.

In this paper, we concentrate our studies on the pinch contribution to the momentum flux which is proportional to the flow velocity and affects the radial profile of the flow. While most theoretical studies on a momentum pinch driven by ITG turbulence were performed in the fluid regime where ∇T_i exceeds the critical value considerably, ∇T_i at the core of many experiments does not deviate much from the threshold value [1]. Therefore, momentum pinch derived from ITG turbulence near marginality can be more relevant to experiments than those derived from fluid description. We also note that theoretical progress has been made in a simple slab geometry [20]. Needless to say, an extension to toroidal geometry is needed. In particular, it is of great physical interest to find out how the ∇B-driven turbulent equipartition (TEP) pinch [21, 22, 23] is modified for the relevant regime of ITG turbulence near marginality where kinetic effects including wave-particle resonant interaction play a crucial role.

In general, the nondiffusive flux of momentum should include the residual stress in addition to pinch. The residual stress does not depend on the flow velocity or the flow velocity shear. The residual stress can generate rotation of plasmas from the stationary state, and can come from various physics mechanisms including $\langle k_\parallel \rangle$ asymmetry induced by a directional imbalance in the wave population in ITG turbulence [24] caused by $\mathbf{E}\times\mathbf{B}$ shear [25], for instance, by nonresonant wave-particle momentum exchange [20, 26], and from high order polarization effect [27, 28].

From our investigation, we find that the inward turbulent equipartition (TEP) momentum pinch remains as the most robust part of the pinch. In addition, the ion temperature gradient driven momentum flux is inward for typical parameters, while the density gradient driven momentum flux is outward as in the previous kinetic result in slab geometry [20].

The rest of this paper is organized as follows. In section 2, we derive a linear

dispersion relation for the toroidal ITG mode in the presence of a drift resonance to get the linear threshold condition and eigenfrequency. With these results, in section 3, a quasilinear expression for parallel momentum transport is calculated, and further classified into a diffusive part and a pinch part. Finally, conclusions for this paper are drawn in section 4.

2. Linear Dispersion Relation of Toroidal ITG Modes in the presence of Drift Resonance

In general, transport driven by wave-particle interaction depends on the eigenfrequency of the wave. Therefore, in this section, a local dispersion relation is derived for the toroidal ITG instability near marginality in the presence of finite parallel flow. We start from the nonlinear electrostatic gyrokinetic equation in general geometry [29] for ions,

$$\frac{\partial F}{\partial t}+\frac{d\mathbf{R}}{dt}\cdot\nabla F+\frac{dv_\parallel}{dt}\frac{\partial F}{\partial v_\parallel}=0 \tag{1}$$

with

$$\frac{d\mathbf{R}}{dt}=v_\parallel\frac{\mathbf{B}^*}{B^*}+\frac{c\mathbf{b}}{e_iB^*}\times\left(e_i\nabla\langle\langle\delta\phi\rangle\rangle+m_i\mu\nabla B\right) \tag{2}$$

and

$$\frac{dv_\parallel}{dt}=-\frac{\mathbf{B}^*}{m_iB^*}\cdot\left(e_i\nabla\langle\langle\delta\phi\rangle\rangle+m_i\mu\nabla B\right). \tag{3}$$

where $v_\parallel=\mathbf{v}\cdot\mathbf{b}$ is the parallel velocity of ions, $\mathbf{B}^*=\mathbf{B}+\frac{m_ic}{e}\nabla\times v_\parallel\mathbf{b}$, $B^*\equiv\mathbf{b}\cdot\mathbf{B}^*$, $\mu=v_\perp^2/2B$ is the magnetic moment, $\delta\phi$ is the fluctuating electrostatic potential, $\mathbf{b}=\mathbf{B}/B$ is the unit vector along the magnetic field, and the double bracket $\langle\langle\cdot\rangle\rangle$ means the gyro-averaged value of the inserted quantity. The $v_\parallel\mathbf{B}^*$ term in equation (2) includes not only the parallel motion of the particle but also the curvature drift. Both the curvature and the ∇B drift terms are pertinent to the aim of this paper.

Linearization of the gyrokinetic equation yields the following perturbed distribution function for ions in Fourier space,

$$\delta f_{i,\mathbf{k}}=-\frac{\frac{c}{B^*}J_0\delta\phi_{\mathbf{k}}k_\vartheta\partial_rF_0+\left(\frac{e}{m}k_\parallel J_0\delta\phi_{\mathbf{k}}+v_\parallel\omega_{d\parallel\mathbf{k}}\frac{eJ_0\delta\phi_{\mathbf{k}}}{T_{i\parallel}}\right)\frac{\partial F_0}{\partial v_\parallel}}{\omega_{\mathbf{k}}-k_\parallel v_\parallel-\omega_{curv\mathbf{k}}-\omega_{\nabla B\mathbf{k}}+i\epsilon^+}, \tag{4}$$

where $\delta f=F-F_0$ is the fluctuating distribution function, $k_\vartheta\equiv\mathbf{b}\times\hat{\mathbf{r}}\cdot\mathbf{k}$, $\partial_r=\hat{\mathbf{r}}\cdot\nabla$, $J_0=J_0(k_\perp\rho_i)$ is the Bessel function, $\omega_{curv\mathbf{k}}\equiv\frac{cmv_\parallel^2}{eB}\mathbf{b}\times(\mathbf{b}\cdot\nabla)\mathbf{b}\cdot k\equiv\xi_{curv\mathbf{k}}v_\parallel^2$ is the curvature drift frequency of ions, $\omega_{d\parallel\mathbf{k}}=\omega_{curv\mathbf{k}}(v_{T\parallel i})=\frac{cT_\parallel}{eB}\mathbf{b}\times(\mathbf{b}\cdot\nabla)\mathbf{b}\cdot k$ is the curvature drift frequency of thermal ions, $\omega_{\nabla B\mathbf{k}}\equiv\frac{cm\mu}{eB}\mathbf{b}\times\nabla B\cdot\mathbf{k}\equiv\mu B\xi_{\nabla B\mathbf{k}}$ is the ∇B drift frequency of ions, $\rho_i\equiv v_{Ti}/\Omega_{ci}$ is the ion Larmor radius, $v_{Ti}\equiv\sqrt{T_i/m_i}$ is the ion thermal velocity and ϵ^+ is due to causality. In this paper, we use a set of variables (r,θ,ζ) to denote the radial, poloidal, and toroidal coordinates, respectively. Note that in a low-β, high aspect ratio torus, the relation $\mathbf{b}\times(\mathbf{b}\cdot\nabla)\mathbf{b}\simeq\mathbf{b}\times\nabla\ln B$ yields $\xi_{curv\mathbf{k}}\simeq\xi_{\nabla B\mathbf{k}}\equiv\xi_{D\mathbf{k}}$ in the lowest order. ∇F_0 contains the free energy source

in configuration space in terms of gradients of macroscopic quantities such as ∇T_i and ∇n_0. Assuming that equilibrium distribution function is a shifted-Maxwellian,

$$F_0(\mathbf{R}, v_\parallel, \mu, t) = n_0(\mathbf{R})(2\pi v_{T\parallel i})^{-1/2}(2\pi v_{T\perp i})^{-1} \exp\left(-\frac{m_i(v_\parallel - U_\parallel)^2/2}{T_{i\parallel}} - \frac{m_i \mu B}{T_{i\perp}}\right),$$

$\partial_r F_0$ and $\frac{\partial F_0}{\partial v_\parallel}$ can be written as

$$\partial_r F_0 = \left\{ \left[1 + \left(\frac{\frac{1}{2} m_i (v_\parallel - U_\parallel)^2}{T_{i\parallel}} - \frac{1}{2} \right) \eta_{i\parallel} + \left(\frac{\mu m_i B}{T_{i\perp}} - 1 \right) \eta_{i\perp} \right] \partial_r \ln n_0 - \frac{\mu m_i}{T_{i\perp}} \partial_r B \right.$$
$$\left. + \frac{m_i (v_\parallel - U_\parallel)}{T_{i\parallel}} \partial_r U_\parallel \right\} F_0,$$

and

$$\frac{\partial F_0}{\partial v_\parallel} = -\frac{m_i (v_\parallel - U_\parallel)}{T_{i\parallel}} F_0,$$

where $n_0(\mathbf{R})$ is the equilibrium density in the guiding center coordinate, $\eta_i = \partial_r \ln T_0 / \partial_r \ln n_0$ and its additional subscript differentiates temperature in parallel direction from that in perpendicular direction. For the perturbed distribution function of electrons, we assume adiabatic response to focus primarily on the ion drift resonance effect on ITG instability :

$$\delta f_e(\mathbf{x}) = \frac{e\delta\phi(\mathbf{x})}{T_{e\parallel}} F_{e0}.$$

Note that $\mathbf{x}$ represents particle position, while $\mathbf{R} = \mathbf{x} - \boldsymbol{\rho}$ denotes guiding center position. Taking into account of the polarization density [30], $n_i^{pol}(\mathbf{x}) = -n_0(1-\Gamma_0)e\delta\phi/T_{i\perp}$ [31], the quasi-neutrality condition gives the following dispersion relation,

$$\frac{n_0 e\delta\phi}{T_{i\parallel}} \left[\frac{1}{\tau_\parallel} + \frac{T_{i\parallel}}{T_{i\perp}} + \Gamma_0 \left(1 - \frac{T_{i\parallel}}{T_{i\perp}} \right) \right] - 2\pi \int B^* \delta h J_0 d\mu dv_\parallel = 0, \tag{5}$$

where $\tau_\parallel = T_{e\parallel}/T_{i\parallel}$ is the ratio of electron to ion parallel temperature, $\Gamma_0 = \Gamma_0(b) = I_0(b)e^{-b}$, $b = k_\perp^2 \rho_i^2$, and $\delta h = \delta f_i + (eJ_0\delta\phi/T_{i\parallel})F_0$ is a nonadiabatic part of guiding center perturbed distribution function which can be written explicitly as

$$\delta h = \left[\omega_{\mathbf{k}} - k_\parallel U_\parallel - \omega_{*Ti} - \left(1 - \frac{T_{i\parallel}}{T_{i\perp}} \right) \omega_{\nabla B\mathbf{k}} - M_\parallel \left(\frac{v_\parallel}{v_{Ti\parallel}} - M_\parallel \right) \omega_{\nabla U} \right.$$
$$\left. - M_\parallel \frac{v_\parallel}{v_{Ti\parallel}} \omega_{d\parallel\mathbf{k}} \right] \left[\omega_{\mathbf{k}} - k_\parallel v_\parallel - \omega_{curv\mathbf{k}} - \omega_{\nabla B\mathbf{k}} + i\epsilon^+ \right]^{-1} \frac{eJ_0\delta\phi}{T_{i\parallel}} F_0, \tag{6}$$

where $\omega_{*Ti} = \frac{v_{Ti\parallel}^2}{\Omega} \mathbf{b} \times \nabla \ln n_0 \cdot \mathbf{k} \left[1 + \left(\frac{\frac{1}{2} m (v_\parallel - U_0)^2}{T_{i\parallel}} - \frac{1}{2} \right) \eta_{i\parallel} + \left(\frac{\mu m B}{T_{i\perp}} - 1 \right) \eta_{i\perp} \right]$ and $M_\parallel = U_\parallel / v_{Ti\parallel}$ is the Mach number defined with parallel temperature.

Several authors have studied the details of drift resonance in the kinetic regime [32, 33, 34, 35]. In this paper, we adopt the constant energy resonance approximation (CERA) [35] to facilitate the integral in equation (5) analytically. Following the CERA, replacement of $v_\perp^2 + 2v_\parallel^2$ by $\frac{4}{3}(v_\perp^2 + v_\parallel^2)$ leads to $\omega_{curv} + \omega_{\nabla B} = \frac{2}{3}\xi_{D\mathbf{k}}(v_\parallel^2 + v_\perp^2)$ with an assumption of low-β and high aspect ratio toroidal geometry. In addition, $k_\parallel v_\parallel < \omega_{curv}, \omega_{\nabla B}$ is assumed to concentrate on studying the effect of drift resonance,

which limits the valid region of the dispersion relation in the **k**-space roughly to $|k_\parallel/k_\theta| < \rho_i/R$, where R is major radius. In this sense, we are only considering a simplified version of toroidal ITG mode, since $k_\parallel \sim 1/R$ for the typical ballooning mode structure. The opposite limit keeping the transit resonance $\omega_{\mathbf{k}} \sim k_\parallel v_\parallel$ has been studied in [36]. We also assume isotropic temperature $T_i \equiv T_{i\parallel} = T_{i\perp}$, low Mach number $M^2 \ll 1$, and negligible finite Larmor radius effect $k_\perp \rho_i \ll 1$. After normalizing the velocity with respect to v_{Ti}, i.e, $v/v_{Ti} \to v$, the equation (5), reduces to

$$\sqrt{\frac{2}{\pi}}\int_0^\infty dv \frac{v^2}{v^2 - \frac{3\omega_{\mathbf{k}}}{2\xi_{D\mathbf{k}} v_{Ti}^2}} e^{-\frac{v^2}{2}} \left\{ \frac{3\omega_{\mathbf{k}}}{2\xi_{D\mathbf{k}} v_{Ti}^2} - \frac{3}{2}\frac{\partial_r \ln n_0}{\partial_r \ln B}\left[1 + \left(\frac{1}{2}v^2 - \frac{3}{2}\right)\eta_i\right]\right\} + \frac{1}{\tau} + 1 = 0. \tag{7}$$

Note that Re(ω) must have a negative sign to allow drift resonance, taking into account of the fact that $\xi_{D\mathbf{k}} < 0$ at the outside midplane where the fluctuation is believed to be stronger. With Plemelj formula, a condition $Im\{\text{equation (7)}\} = 0$ determines the resonance frequency at marginality,

$$\alpha_c = \frac{\frac{3}{2}\eta_i - 1}{\eta_i - \frac{4}{3}\frac{L_n}{R}}, \tag{8}$$

where the normalized frequency α_c is defined as $\alpha_c \equiv \frac{3\omega_{\mathbf{k}}}{4\xi_{D\mathbf{k}} v_{Ti}^2}$, $L_n = (-\partial_r \ln n_0)^{-1}$ is the density scale length and $\partial_r \ln B \simeq -1/R$. We can observe that the negative frequency condition sets the minimum bound of η_i value at marginality. For instance, $\eta_i > \frac{2}{3}$ is a necessary condition for a nonrotating plasma. Substituting this eigenfrequency at marginality into $Re\{\text{Equation (7)}\} = 0$, the following ITG threshold can be obtained with consideration of the negative frequency condition,

$$\left.\frac{R}{L_{Ti}}\right|_{Thres} = \text{Max}\left[\frac{4}{3}\left(1 + \frac{1}{\tau}\right), \frac{2}{3}\frac{R}{L_n}\right] \tag{9}$$

where $L_{Ti} = (-\partial_r \ln T_i)^{-1}$ is scale length of the temperature gradient. This agrees with the result by Romanelli [34] as it should. We note that lower temperature ratio has stabilizing effect on instability threshold in agreement with results of several theoretical studies [34, 36, 37].

Now we compare the threshold values from theoretical models with experimental data from TFTR [1] in Figure 1. Here, we've used the electron density profile in the definition of η_i to obtain the threshold in the absence of available data on impurity ion and beam ion density values, while the main ion density was used in [1] (for instance, for figure 1). In addition, the threshold value for ∇ B model [34] is considered as another approximation in the same regime of CERA in k-space where the drift resonance is dominant over the transit resonance. In this approximation, we replace $v_\perp^2 + 2v_\parallel^2$ by $2v_\perp^2$ in the wave-particle resonant integral. The following formula is the threshold value for ∇B model [34],

$$\left.\frac{R}{L_{Ti}}\right|_{Thres} = \text{Max}\left[2\left(1 + \frac{1}{\tau}\right), \frac{R}{L_n}\right]. \tag{10}$$

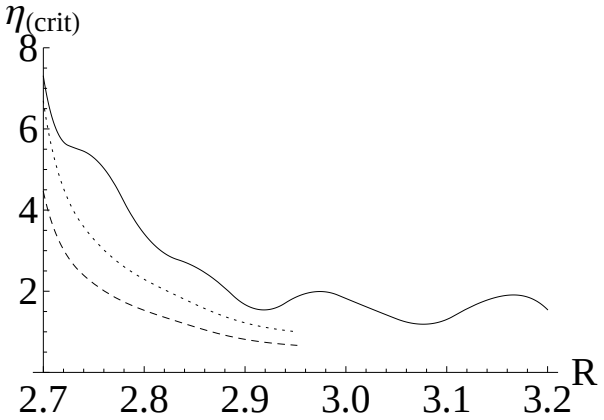

Figure 1. Comparison of η_i from TFTR experiment with theoretical predictions for η_{crit}. The solid line (——) corresponds to results from a TFTR experiment, the dotted line (· · · · · ·) corresponds to results from the ∇B model, and the dashed line (- - - -) corresponds to results from the Constant Energy Resonance Approximation(CERA). The theoretically estimated lines are plotted only in the domain satisfying the drift resonance condition $\omega < 0$ on the bad curvature side.

Even with these caveats, Figure 1 illustrates that in reality the experimental η_i value does not deviate significantly from the threshold of instability confirming the conclusion of [1]. Since the wave-particle resonant interaction is important near marginality, a kinetic approach is necessary to evaluate transport accurately for realistic parameters including the stiff ion temperature profile. We note that some gyrokinetic simulations [38] indicate strong wave-particle resonant interaction even away from marginality.

3. Momentum Pinch and Diffusion

The turbulent parallel momentum density flux driven by electrostatic fluctuations in the quasilinear regime can be written as

$$\Gamma_\parallel = \langle \delta(nmU_\parallel)\delta v_r \rangle \approx mU_\parallel \langle \delta n \delta v_r \rangle + nm \langle \delta U_\parallel \delta v_r \rangle \equiv mU_\parallel \Gamma_n + \Pi_{r,\parallel} \tag{11}$$

where Γ_n is the turbulent particle flux and $\Pi_{r,\parallel}$ is the Reynolds stress corresponding to parallel flow fluctuations carried by radial velocity fluctuations. Here, we assume that the $\mathbf{E}\times\mathbf{B}$ drift caused by electric potential fluctuations is the radial velocity fluctuation responsible for transport. The first term on the RHS of equation (11) is a contribution of the turbulent particle flux to the turbulent parallel momentum density flux. This contribution vanishes for the adiabatic electron response considered in this paper. The second term is due to the parallel momentum flux contribution of the Reynolds stress in the radial direction.

The Reynolds stress component which is the parallel fluctuating flow carried by radial velocity fluctuations is traditionally divided into three components [20],

$$\langle \delta U_\parallel \delta v_r \rangle = -\chi_\parallel \frac{dU_\parallel}{dr} + V_{pinch} U_\parallel + \Pi_{r,\parallel}^{Res} \tag{12}$$

where the first term on the RHS is the momentum diffusion driven by the gradient of the flow, the second term is a pinch term proportional to the flow velocity, and the last term is the residual stress which depends on other macroscopic quantities such as $\nabla n_0, \nabla T_i, \nabla T_e$, etc. The diffusion, pinch and residual stress are generally classified according to their proportionality to the gradient of the transported quantity, the transported quantity itself, and the rest which cannot be characterized by the aforementioned two categories, respectively. Therefore, this semi-phenomenological classification is quasi-local in nature. From this equation we can deduce that the only term able to generate rotation of plasma from the stationary state is the residual stress. In other words, the residual stress is a key ingredient of intrinsic rotation. This residual stress can be obtained from $\langle k_\parallel \rangle$ asymmetry induced by a directional imbalance in the wave population in ITG turbulence [24] caused by $\mathbf{E} \times \mathbf{B}$ shear [25], for instance, by nonresonant wave-particle momentum exchange [20], or by curvature effects in the stress tensor [39], and from high order polarization effects [27, 28]. A strong correlation among $\langle k_\parallel \rangle$ asymmetry, zonal flow shear, and inward momentum flux has been observed in GTS simulations [40], suggesting the existence of residual stress. A similar conclusion has been drawn from a different simulation [41]. Then, equation (11) reduces to

$$\Gamma_\parallel = nm\langle \delta U_\parallel \delta v_r \rangle = nm\left(-\chi_\parallel \frac{dU_\parallel}{dr} + V_{pinch} U_\parallel + \Pi_{r,\parallel}^{Res} \right), \tag{13}$$

where χ_u is the diffusion coefficient for parallel flow, V_{pinch} is the pinch velocity, and finally $\Pi_{r,\parallel}^{Res}$ is the residual stress.

With this background, this section is devoted to explicitly evaluating the diffusion coefficient and the pinch velocity for the turbulent angular momentum density flux within the quasilinear approximation, thus elucidating the dependency of these terms on plasma parameters. We'll address the residual stress, which can be crucial in more general context [42, 43], in the future.

The turbulent angular momentum density flux is written in terms of the perturbed distribution function of ions, δf_i, as

$$\Gamma_\parallel \equiv 2\pi \int d\mu dv_\parallel \langle B^* m_i R v_\parallel \delta f_i \delta v_r \rangle. \tag{14}$$

Here, $\langle \cdots \rangle$ is an ensemble average approximated by the flux surface average. By substituting the gyrokinetic perturbed distribution function in equation (4) into equation (14) with the CERA, we can obtain an analytic formula for the angular momentum density flux in the quasilinear regime,

$$\begin{aligned}
\Gamma_\parallel &= \sum_{\mathbf{k}} |\delta v_{r\mathbf{k}}|^2 \frac{1}{|\omega_{D\mathbf{k}}|} \sqrt{\pi} \alpha_c^{\frac{3}{2}} e^{-\alpha_c} \Bigg\{ -\partial_r (n_0 m_i R U_\parallel) \\
&\qquad + \left[\left(\frac{5}{2} - \alpha_c \right) \partial_r \ln T_i + \left(-2 + \frac{8}{5}\alpha_c \right) \partial_r \ln B \right] n_0 m_i R U_\parallel \Bigg\} \qquad (15) \\
&= \sum_{\mathbf{k}} |\delta v_{r\mathbf{k}}|^2 \frac{1}{|\omega_{D\mathbf{k}}|} \sqrt{\pi} \alpha_c^{\frac{3}{2}} e^{-\alpha_c} \Bigg\{ -n_0 m_i R^2 \partial_r \omega_\parallel + \Bigg[-\partial_r \ln n_0
\end{aligned}$$

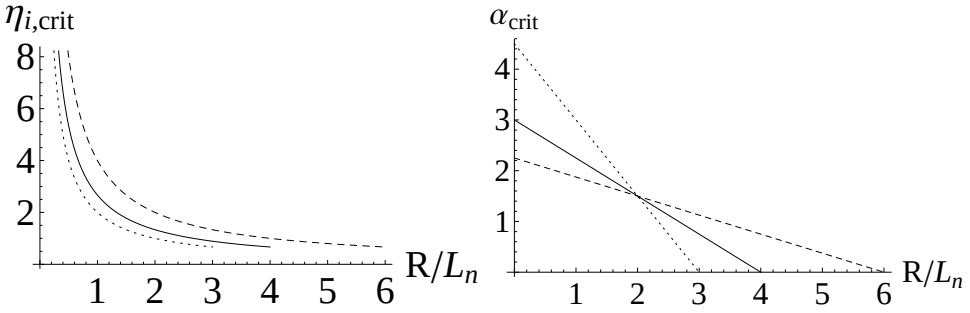

Figure 2. Parametric dependence of (a) threshold $\eta_{i,crit}$ for the electron temperature to ion temperature ratio $\tau \equiv \frac{T_e}{T_i} = 0.5$ (- - - -), 1 (——), and 2 ($\cdots\cdots$), and (b) the corresponding normalized eigenfrequency α_{crit}.

$$+\left(\frac{5}{2}-\alpha_c\right)\partial_r \ln T_i + \frac{8}{5}\alpha_c \partial_r \ln B\Bigg] n_0 m_i R^2 \omega_\parallel \Bigg\}. \tag{16}$$

The following diffusion coefficients and pinch velocities can be identified as,

$$\chi^L_{Ang} = \sum_{\mathbf{k}} |\delta v_{r\mathbf{k}}|^2 \frac{1}{|\omega_{D\mathbf{k}}|}\sqrt{\pi}\alpha_c^{\frac{3}{2}} e^{-\alpha_c}, \tag{17a}$$

$$V^L_{r,Ang} = \sum_{\mathbf{k}} |\delta v_{r\mathbf{k}}|^2 \frac{1}{|\omega_{D\mathbf{k}}|}\sqrt{\pi}\alpha_c^{\frac{3}{2}} e^{-\alpha_c}\left[\left(\frac{5}{2}-\alpha_c\right)\partial_r \ln T_i + \left(-2+\frac{8}{5}\alpha_c\right)\partial_r \ln B\right], \tag{17b}$$

$$\frac{V^L_{r,Ang}}{\chi^L_{Ang}} \simeq \left(\frac{5}{2}-\alpha_c\right)\partial_r \ln T_i + \left(-2+\frac{8}{5}\alpha_c\right)\partial_r \ln B, \tag{17c}$$

using equation (15) with angular momentum density as a main independent variable in the flux-gradient relation. A common factor $\alpha_c^{3/2} e^{-\alpha_c}$ is proportional to the number of ions resonant with toroidal ITG.

On the other hand, if we use the angular rotation frequency, $\omega_\parallel$, as a main independent variable, we obtain

$$\chi^\omega_{Ang} = \sum_{\mathbf{k}} |\delta v_{r\mathbf{k}}|^2 \frac{1}{|\omega_{D\mathbf{k}}|}\sqrt{\pi}\alpha_c^{\frac{3}{2}} e^{-\alpha_c}, \tag{18a}$$

$$V^\omega_{r,Ang} = \sum_{\mathbf{k}} |\delta v_{r\mathbf{k}}|^2 \frac{1}{|\omega_{D\mathbf{k}}|}\sqrt{\pi}\alpha_c^{\frac{3}{2}} e^{-\alpha_c}\left[-\partial_r \ln n_0 + \left(\frac{5}{2}-\alpha_c\right)\partial_r \ln T_i + \frac{8}{5}\alpha_c \partial_r \ln B\right], \tag{18b}$$

$$\frac{V^\omega_{r,Ang}}{\chi^\omega_{Ang}} \simeq -\partial_r \ln n_0 + \left(\frac{5}{2}-\alpha_c\right)\partial_r \ln T_i + \frac{8}{5}\alpha_c \partial_r \ln B. \tag{18c}$$

The gradients of these two quantities are related via $\partial_r(n_0 m_i R^2 \omega_\parallel) \simeq n_0 m_i R^2 \omega_\parallel \left(\partial_r \ln n_0 + \partial_r \ln \omega_\parallel - 2\partial_r \ln B\right)$ on the assumption that magnetic field strength is proportional to inverse of major radius. Here, $\delta v_{r\mathbf{k}} \equiv -i\frac{ck_\vartheta \delta\phi}{B}$ is the $\mathbf{E}\times\mathbf{B}$ radial fluctuation velocity, $\omega_{D\mathbf{k}} \equiv v_{Ti}^2 \xi_{D\mathbf{k}}$ is the thermal drift frequency. Note that the drift resonance at the low field side can occur for $\alpha_c > 0$.

It is clear from equation (18b) that the density gradient driven flux is outward while the magnetic field gradient pinch is inward. However, direction of the temperature

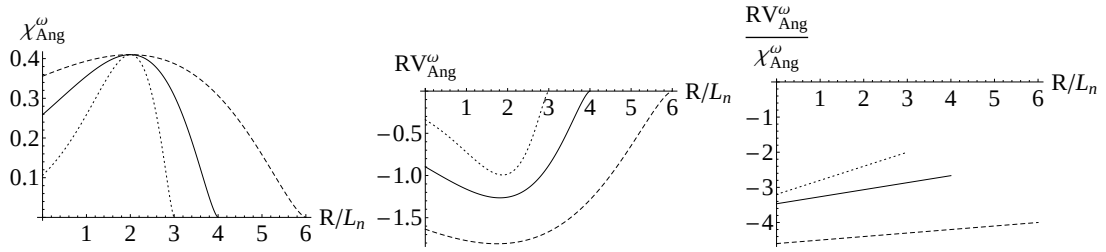

Figure 3. Parametric dependence of (a) angular momentum diffusivity χ_{Ang}, (b) pinch velocity RV^{ω}_{Ang}, and (c) their corresponding pinch velocity to angular momentum diffusivity ratio $\frac{RV^{\omega}_{Ang}}{\chi_{Ang}}$ for $\tau \equiv \frac{T_e}{T_i} = 0.5$ (- - - -), 1 (——), and 2 ($\cdots\cdots$). The units for both χ_{Ang} and RV^{ω}_{Ang} are $\frac{\sqrt{\pi}|\delta v_{r\mathbf{k}}|^2}{|\omega_D|}$.

gradient driven pinch depends on the eigenfrequency which needs to be determined from the dispersion relation. In Figure 2, the dependence of the threshold value of η_i on R/L_n is presented as a function of ion to electron temperature ratio by use of equation (9). Based on these threshold values, we can obtain the normalized eigenfrequency α_{crit} at the threshold value $\eta_{i,crit}$ from equation (8). Note that within our model, $\eta_{i,crit}$ is predicted only for the parameter regime where the drift resonance condition, $\alpha_{crit} > 0$ is satisfied. In addition, a degeneracy point for any value of τ exists at $(R/L_n, \alpha_{crit}) = (2, 1.5)$, which can easily be recognized from equation (8). Since the critical value of α_c for determining the direction of the temperature gradient driven pinch is 5/2, in the region where R/L_n is above the degenerate point value, i.e. for $R/L_n > 2$, the pinch direction due to the temperature gradient is inward regardless of the temperature ratio.

On the other hand, for $R/L_n < 2$, the direction of the pinch depends not only on R/L_n but also on the temperature ratio which changes the slope of the α_{crit} line. Note that the increment of the temperature ratio raises the slope. For example, substituting the threshold condition, equation (9), into the eigenfrequency equation (8), we can find a critical temperature ratio $\tau_{crit} = 2/3$. For τ above the critical value, the temperature gradient driven pinch must change its direction for $R/L_n \leq 2$, i.e., near the flat density region. This outward pinch driven by the temperature gradient can occur if $\alpha_c > 2.5$. However, we should note that, for that parameter regime, the number of resonant ions becomes exponentially small, and so as the flux (both diffusion and pinch). Hence, practically speaking, the temperature gradient driven pinch carried by resonant particles is inward when it's significant enough to be relevant. This feature is qualitatively similar, but not identical, to the kinetic result in slab geometry where the temperature gradient driven pinch direction is always inward when ITG is linearly unstable [20].

In summary, we've investigated the direction of each pinch contribution driven by various gradients and carried by ions resonant with ITG near marginality. The density gradient driven pinch is always outward while the magnetic field gradient driven pinch, which can be regarded as a kinetic extension of the TEP pinch, is always inward and relatively robust under a change of parameters. Note that the physics of the TEP pinch coming from the compressibility of the perturbed $\mathbf{E} \times \mathbf{B}$ velocity associated with the

Table 1. Analytic Predictions on Momentum Pinch. $\eta_i^{crit} = 2[1 + 2b(1 - I_1/I_0)]^{-1}$, $\Omega = (\omega_{\mathbf{k}} - k_\theta \langle v_{\mathbf{E}\times\mathbf{B}} \rangle - k_\parallel \langle v_\parallel \rangle)/\sqrt{2} k_\parallel v_{Ti}$, and $\alpha_c = -3\omega_{\mathbf{k}}/4\omega_{D\mathbf{k}} > 0$

For ITG : V_{pinch}/χ_ϕ	∇n driven	∇T_i driven	∇B driven
Fluid Regime in Torus [47]	$-1/L_n$ Inward	0	$-4/R$ [21], for $\tau = 1$ Inward
Kinetic Regime near Marginality in Slab [20]	$1/L_n$ Outward	$-\left(\frac{1}{\eta_i^{crit}} + \Omega^2\right)/L_{Ti}$ Inward	Ignored
Kinetic Regime near Marginality in Torus (This work)	$1/L_n$ Outward	$-\left(\frac{5}{2} - \alpha_c(\omega_{\mathbf{k}})\right)/L_{Ti}$ Inward	$-\frac{8}{5}\alpha_c(\omega_{\mathbf{k}})/R$ Inward

magnetic field strength inhomogeneity is most clearly illustrated in the fluid regime [21, 22, 23, 44, 45, 46]. Finally, the temperature gradient driven pinch is generally inward except near the flat density regime where the direction strongly depends on the temperature ratio between ions and electrons.

Analytic progress has been made in calculating the pinch in a torus [21, 47]. Based on the moment approach from the gyrokinetic equation conserving phase space volume [29], it was shown that the pinch can be generally classified into two categories, the Turbulent Equipartition Pinch(TEP) and the Curvature driven THermoelectric pinch(CTH) [21]. Even though this classification is most transparent in the fluid regime, it can be applied in the kinetic regime based on the gradients which drive that part of the pinch. In the case of the TEP pinch, ∇B is the relevant quantity in a sense that the compressibility of $\mathbf{E} \times \mathbf{B}$ flows plays an essential role in the TEP mechanism [27, 22, 23]. On the other hand, pinch driven by ∇n_0 or ∇T_i should be classified as the CTH pinch. With this classification, the first and second terms in equation (18b) proportional to density and temperature gradient respectively can be identified as CTH pinch, and the last term proportional to the magnetic field gradient as TEP pinch. Note that α_c, which appears in the coefficients has a weak parametric dependence on R, as $\alpha_c \simeq \frac{\frac{3}{2}\eta_i - 1}{\eta_i(1 - \frac{4}{3}\frac{L_{Ti}}{R})} \simeq \frac{3}{2} + O(\frac{L_{Ti}}{R}, \eta_i^{-1})$.

Some remarks are in order for the diffusion coefficient and pinch velocity of angular momentum density flux in the presence of drift resonance. First of all, both the diffusion coefficient and the pinch velocity are proportional to $\alpha_c^{3/2} e^{-\alpha_c}$ (i.e, number of resonant ions) which has a maximum at $\alpha_c = 3/2$. This reflects drift resonance yields maximum transport at the certain frequency while its effect vanishes as $\alpha_c \to 0$ or $\alpha_c \to \infty$. In addition, as ω(or α_c) $\to 0$, the pinch velocity vanishes in this simple toroidal limit, while it persists to have a finite value in the slab case [20]. The pinch to diffusion coefficient

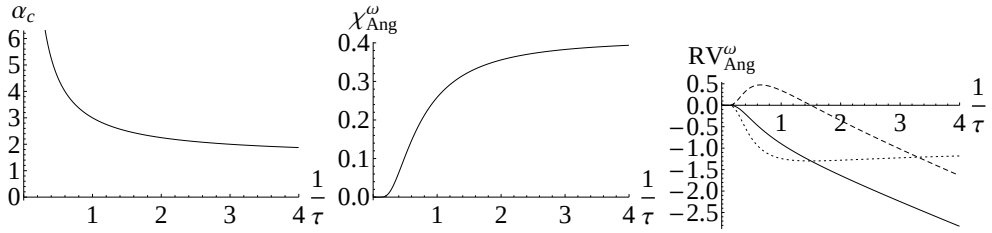

Figure 4. Parametric dependence of (a) normalized eigenfrequency α_c, (b) angular momentum diffusivity χ^{ω}_{Ang} and (c) pinch velocity RV^{ω}_{Ang} for flat density profile. The units for both quantities are $\frac{\sqrt{\pi}|\delta v_{r\mathbf{k}}|^2}{|\omega_D|}$. In (c), contributions of CTH and TEP pinch for total pinch are presented. The dotted line ($\cdots\cdots$) corresponds to TEP pinch (RV^{TEP}_{Ang}), the dashed line (- - - -) corresponds to CTH pinch (RV^{CTH}_{Ang}) and the solid line (——) corresponds to total pinch ($RV_{Ang} = RV^{TEP}_{Ang} + RV^{CTH}_{Ang}$).

ratio in this case is,

$$\frac{V^{\omega}_{r,Ang}}{\chi^{\omega}_{Ang}} \simeq \frac{1}{L_n} - \left(\frac{5}{2} - \alpha_c\right)\frac{1}{L_{Ti}} - \frac{8}{5}\alpha_c\frac{1}{R}.$$

The direction of density gradient driven pinch in kinetic regime is outward in both slab [20] and torus, in contrast to an inward pinch obtained in the fluid regime [47], for pure ITG instability.

Even though the lower temperature ratio has stabilizing effect on η_{crit} threshold values, they increase the absolute values of pinch velocity and diffusion coefficient. Figure 3 shows parametric dependence of diffusivity, pinch velocity, and their ratio with respect to the electron to ion temperature ratio. The pinch to diffusivity ratio increases as the temperature ratio decreases. Various analytic predictions on the pinch to diffusion ratio from ITG turbulence are summarized in table 1.

In the flat density regime, the equation (8) reduces to $\alpha_c = \frac{3/2}{1-\frac{4}{3}\frac{L_{Ti}}{R}}$, and corresponding pinch velocity and diffusion coefficient are calculated as a function of $1/\tau$, presented in Figure 4. It is clear that below certain value of $1/\tau$, the large eigenfrequency makes both pinch and diffusion, which are proportional to $\alpha_c^{3/2}e^{-\alpha_c}$, negligible. We would like to remark that the direction of total pinch consisting of TEP pinch and CTH pinch is always inward for the flat density profile because the inward TEP pinch is robust enough that it dominates the outward CTH pinch which can occur in a certain regime. As mentioned before, the CTH pinch can change its direction depending on parameters, whereas TEP pinch is always inward.

4. Conclusion

In this paper, an analytic dispersion relation for the ion temperature gradient instability in a simple toroidal limit ($\omega_{\mathbf{k}}, \omega_{D\mathbf{k}} \gg k_{\parallel}v_{\parallel}$) has been obtained from a kinetic calculation with the CERA. Based on the dispersion relation, the parallel momentum flux, and its corresponding diffusion coefficient and pinch velocity have been estimated analytically

from a quasilinear calculation based on the gyrokinetic equation. In addition, the pinch velocities are classified into the TEP pinch and the CTH pinch according to their dependence on the gradients of the macroscopic quantities. Our results show that the inward turbulent equipartition (TEP) momentum pinch remains as the most robust part of pinch. Ion temperature gradient driven momentum flux is inward for typical parameters, while density gradient driven momentum flux is outward as in the previous kinetic result in slab geometry.

Acknowledgments

We thank P.H. Diamond for his insightful comments and encouragement. We'd also like to acknowledge useful discussion with S.M. Kaye, J.E. Rice, S.D. Scott, C.S. Chang, X. Garbet, Ö.D. Gürcan, K. Ida, C.J. McDevitt, G. Rewoldt, W.M. Solomon, W.X. Wang and M. Yoshida. This work was supported by the U.S. Department of Energy Contract No. DE-AC02-09-CH11466, and by SciDAC Center for Gyrokinetic Particle Simulation of Turbulent Transport in Burning Plasmas.

References

[1] Scott S.D. *et al* 1990 *Phys. Rev. Lett.* **64** 531
[2] Mattor N. and Diamond P.H. 1988 *Phys. Fluids* **31** 1180
[3] Ida K., Miura Y., Matsuda T., Itoh K., Hidekuma S., Itoh S.I. and Group JFT-2M 1995 *Phys. Rev. Lett.* **74** 1990
[4] Eriksson L-G., Righi E. and Zastrow K-D. 1997 *Plasma Phys. Control. Fusion* **39** 27
[5] Rice J.E., Marmar E.S., Bombarda F. and Qu L. 1997 *Nucl. Fusion* **37** 421
[6] Rice J.E., Bonoli P.T., Goetz J.A., Greenwald M.J., Hutchinson I.H., Marmar E.S., Porkolab M., Wolfe S.M., Wukitch S.J. and Chang C.S. 1999 *Nucl. Fusion* **39** 1175
[7] Hoang G.T. *et al* 2000 *Nucl. Fusion* **40** 913
[8] Hutchinson I.H., Rice J.E., Granetz R.S. and Snipes J.A. 2000 *Phys. Rev. Lett.* **84** 3330
[9] Rice J.E. *et al* 2000 *Phys. Plasmas* **7** 1825
[10] deGrassie J.S., Burrell K.H., Baylor L.R., Houlberg W. and Lohr J. 2004 *Phys. Plasmas* **11** 4323
[11] deGrassie J.S., Burrell K.H., Baylor L.R., Houlberg W. and Solomon W. 2006 *in Proceedings of the 20th IAEA Fusion Energy Conference, Villamoura, 2004 IAEA, Vienna* IAEA-CN-116/EX/6-4Rb (available at http:www-naweb.iaea.org/napc/physics/fec/fec2004/datasets/Ex-64Rb.html).
[12] Sakamoto Y., Ide S., Yoshida M., Fujita T., Takenaga H. and Kamada Y. 2006 *Plasma Phys. Controlled Fusion* **48** A63
[13] Bortolon A., Duval B.P., Pochelon A. and Scarabosio A. 2006 *Phys. Rev. Lett.* **97** 235003
[14] Yoshida M., Koide Y., Takenaga H., Urano H., Oyama N., Kamiya K., Sakamoto Y. and Kamada Y. 2006 *Plasma Phys. Control. Fusion* **48** 1673
[15] Yoshida M., Koide Y., Takenaga H., Urano H., Oyama N., Kamiya K., Sakamoto Y., Matsunaga G., Kamada Y. and the JT-60 Team 2007 *Nucl. Fusion* **47** 856
[16] Solomon W.M., Kaye S.M., Bell R.E., LeBlanc B.P., Menard J.E., Rewoldt G., Wang W., Levinton F.M., Yuh H. and Sabbagh S.A. 2008 *Phys. Rev. Lett.* **101** 065004
[17] Kaye S.M., Solomon W., Bell R.E., LeBlanc B.P., Levinton F., Menard J., Rewoldt G., Sabbagh S., Wang W. and Yuh H. 2009 *Nucl. Fusion* **49** 045010
[18] Solomon W.M. *et al* 2009 *Nucl. Fusion* **49** 085005
[19] Tala T. *et al* 2009 *Phys. Rev. Lett* **102** 075001
[20] Diamond P.H., McDevitt C.J., Gürcan Ö.D., Hahm T.S., Naulin V. 2008 *Phys. Plasmas* **15** 012303

[21] Hahm T.S., Diamond P.H., Gürcan Ö.D., Rewoldt G. 2007 *Phys. Plasmas* **14** 072302
[22] Hahm T.S., Diamond P.H., Gürcan Ö.D., Rewoldt G. 2008 *Phys. Plasmas* **15** 055902
[23] Gürcan Ö.D., Diamond P.H. and Hahm T.S. 2008 *Phys. Rev. Lett.* **100** 135001
[24] Gürcan Ö.D., Diamond P.H., Hahm T.S. and Singh R. 2007 *Phys. Plasmas* **14** 042306
[25] Dominguez R.R. and Staebler G.M. 1993 *Phys. Fluids* **B5** 3876
[26] Diamond P.H., McDevitt C.J., Gürcan Ö.D., Hahm T.S., Wang W.X., Yoon E.S., Holod I., Lin Z., Naulin V. and Singh R. 2009 *Nucl. Fusion* **49** 045002
[27] McDevitt C.J., Diamond P.H., Gürcan Ö.D. and Hahm T.S. 2009 *Phys. Plasmas* **16** 052302
[28] McDevitt C.J., Diamond P.H., Gürcan Ö.D. and Hahm T.S. 2009 *Phys. Rev. Lett.* (in print)
[29] Hahm T.S. 1988 *Phys. Fluids* **31** 2670
[30] Lee W.W. 1983 *Phys. Fluids* **26** 556
[31] Dubin D.H.E., Krommes J.A., Oberman C. and Lee W.W. 1983 *Phys. Fluids* **26** 3524
[32] Terry P., Anderson W. and Horton W. 1982 *Nucl. Fusion* **22** 487
[33] Biglari H., Diamond P.H. and Rosenbluth M.N. 1989 *Phys Fluids* **B1** 109
[34] Romanelli F. 1989 *Phys. Fluids* **B1** 1018
[35] Romanelli F. and Briguglio S. 1990 *Phys. Fluids* **B2** 754
[36] Hahm T.S. and Tang W.M. 1989 *Phys. Fluids* **B1** 1185
[37] Casati A., Bourdelle C., Garbet X. and Imbeaux F. 2008 *Phys. Plasmas* **15** 042310
[38] Holod I. and Lin Z. 2008 *Phys. Plasmas* **15** 092302
[39] Weiland J., Singh R., Nordman H., Kaw P., Peeters A.G. and Strinzi D. 2009 *Nucl. Fusion* **49** 065033
[40] Wang W.X., Hahm T.S., Ethier S, Rewoldt G., Lee W.W., Tang W.M. and Kaye S.M. 2009 *Phy. Rev. Lett.* **102** 035005
[41] Idomura Y., Urano H., Aiba N. and Tokuda S. 2009 *Nucl. Fusion* **49** 065029
[42] Yan Z., Yu J.H., Holland C., Xu M., Müller S.H. and Tynan G.R. 2008 *Phys. Plasmas* **15** 092309
[43] Gürcan Ö.D., Diamond P.H., McDevitt C.J. and Hahm T.S. 2009 *Phys. Plasmas* "A simple model of intrinsic rotation in high confinement regime tokamak plasmas" submitted
[44] Isichenko M.B., Gruzinov A.V. and Diamond P.H. 1995 *Phys. Rev. Lett.* **74** 4436
[45] Naulin V., Nycander J. and Juul Rasmussen J. 1998 *Phys. Rev. Lett.* **81** 4148
[46] Garbet X., Dubuit N., Asp E., Sarazin Y., Bourdelle C., Ghendrih P. and Hoang G.T. 2005 *Phys. Plasmas* **12** 082511
[47] Peeters A.G., Angioni C. and Strintzi D. 2007 *Phys. Rev. Lett.* **98** 265003

The Princeton Plasma Physics Laboratory is operated
by Princeton University under contract
with the U.S. Department of Energy.

Information Services
Princeton Plasma Physics Laboratory
P.O. Box 451
Princeton, NJ 08543

Phone: 609-243-2245
Fax: 609-243-2751
e-mail: pppl_info@pppl.gov
Internet Address: http://www.pppl.gov